Geophysical Research Letters

RESEARCH LETTER
10.1029/2023GL104095

Closing Greenland's Mass Balance: Frontal Ablation of Every Greenlandic Glacier From 2000 to 2020

William Kochtitzky[1,2], Luke Copland[1], Michalea King[3], Romain Hugonnet[4,5,6], Hester Jiskoot[7], Mathieu Morlighem[8], Romain Millan[9], Shfaqat Abbas Khan[10], and Brice Noël[11]

[1]Department of Geography, Environment and Geomatics, University of Ottawa, Ottawa, ON, Canada, [2]School of Marine and Environmental Programs, University of New England-Biddeford Campus, Biddeford, ME, USA, [3]Applied Physics Laboratory, University of Washington, Seattle, WA, USA, [4]LEGOS, Université de Toulouse, CNES, CNRS, IRD, UPS, Toulouse, France, [5]Laboratory of Hydraulics, Hydrology and Glaciology (VAW), ETH Zürich, Zürich, Switzerland, [6]Swiss Federal Institute for Forest, Snow and Landscape Research (WSL), Birmensdorf, Switzerland, [7]Department of Geography & Environment, University of Lethbridge, Lethbridge, AB, Canada, [8]Department of Earth Sciences, Dartmouth College, Hanover, NH, USA, [9]Institut des Géosciences de l'Environnement, CNES, Grenoble, France, [10]DTU Space, Technical University of Denmark, Kongens Lyngby, Denmark, [11]Department of Climatology and Topoclimatology, University of Liège, Liège, Belgium

Key Points:

- Frontal ablation of the Greenland Ice Sheet averaged 510.2 ± 18.6 Gt a^{-1} for 2010–2020, ~90% of which came from ice discharge
- The frontal ablation we measured is larger than the total mass loss from the ice sheet, indicating a positive climatic-basal balance
- Only 16 glaciers account for 50% of the total frontal ablation from the Greenland Ice Sheet

Supporting Information:

Supporting Information may be found in the online version of this article.

Correspondence to:

W. Kochtitzky,
wkochtitzky@une.edu

Citation:

Kochtitzky, W., Copland, L., King, M., Hugonnet, R., Jiskoot, H., Morlighem, M., et al. (2023). Closing Greenland's mass balance: Frontal ablation of every Greenlandic glacier from 2000 to 2020. *Geophysical Research Letters*, *50*, e2023GL104095. https://doi.org/10.1029/2023GL104095

Received 13 APR 2023
Accepted 31 JUL 2023

Author Contributions:

Conceptualization: William Kochtitzky, Luke Copland, Michalea King, Hester Jiskoot
Data curation: William Kochtitzky, Romain Hugonnet, Mathieu Morlighem, Romain Millan, Shfaqat Abbas Khan, Brice Noël
Formal analysis: William Kochtitzky, Romain Hugonnet
Funding acquisition: William Kochtitzky, Luke Copland
Investigation: William Kochtitzky, Luke Copland, Michalea King, Hester Jiskoot

Abstract In Greenland, 87% of the glacierized area terminates in the ocean, but mass lost at the ice-ocean interface, or frontal ablation, has not yet been fully quantified. Using measurements and models we calculate frontal ablation of Greenland's 213 outlet and 537 peripheral glaciers and find a total frontal ablation of 481.8 ± 24.0 for 2000–2010 and 510.2 ± 18.6 Gt a^{-1} for 2010–2020. Ice discharge accounted for ~90% of frontal ablation during both periods, while mass loss due to terminus retreat comprised the remainder. Only 16 glaciers were responsible for the majority (>50%) of frontal ablation from 2010 to 2020. These estimates, along with the climatic-basal balance, allow for a more complete accounting of Greenland Ice Sheet and peripheral glacier mass balance. In total, Greenland accounted for ~90% of Northern Hemisphere frontal ablation for 2000–2010 and 2010–2020.

Plain Language Summary We estimate the mass of ice lost from all Greenland glaciers that entered the ocean during each of the last two decades. This ice loss at the front of these marine-terminating glaciers is called frontal ablation and is approximately equal to the mass of icebergs entering the ocean. Frontal ablation is important because 87% of glacier area in Greenland ends in the ocean, through 750 outlets, and previous work has only approximated frontal ablation. This study quantifies it for the first time, helping to close the mass budget for the Greenland Ice Sheet and better partition its mass balance into components. We find that Greenland accounts for ~90% of all Northern Hemisphere frontal ablation and, of that contribution, just 17 glaciers for 2000–2010 and 16 glaciers for 2010–2020 account for more than half of total Greenland frontal ablation.

1. Introduction

Globally, glaciers and ice sheets have been losing mass at accelerated rates during the 21st century, with the most rapid changes occurring at glaciers that terminate in the ocean (Hugonnet et al., 2021; IPCC, 2021; Khan et al., 2022; King et al., 2018; Mankoff et al., 2020). Greenland is likely to become the primary contributor to global sea level rise by 2100, with projected contributions of between 32 and 90 mm, depending on future warming and carbon emissions (Goelzer et al., 2020). The negative mass balance of the Greenland Ice Sheet and peripheral glaciers (hereafter Greenland) have already contributed 0.35 mm a^{-1} (very likely range of 0.23–0.46 mm a^{-1}) to sea level rise from 1901 to 2018, for a total of 40.4 mm (IPCC, 2021). Mass balance consists of two components: climatic-basal mass balance and frontal ablation (Cogley et al., 2011). Climatic-basal mass balance includes annual accumulation and ablation occurring at the glacier surface, within the glacier, and at the bed (Cogley et al., 2011; Karlsson et al., 2021), which for land-terminating glaciers is the entire mass balance. For lake and marine-terminating glaciers, frontal ablation occurs in addition and is the process of mass loss at a typically near-vertical glacier margin (i.e., terminus or calving cliff) including calving, subaerial melting, subaerial sublimation, and subaqueous melting (Cogley et al., 2011), and must be added to the climatic-basal balance to

Methodology: William Kochtitzky, Luke Copland, Michalea King, Romain Hugonnet
Resources: Michalea King
Supervision: Luke Copland
Visualization: William Kochtitzky
Writing – original draft: William Kochtitzky, Luke Copland
Writing – review & editing: William Kochtitzky, Luke Copland, Michalea King, Romain Hugonnet, Hester Jiskoot, Mathieu Morlighem, Romain Millan, Shfaqat Abbas Khan, Brice Noël

determine the total mass balance. The climatic mass balance for Greenland has been calculated by several studies (Fettweis et al., 2020; Noël et al., 2018), but frontal ablation has only been computed for Greenland peripheral glaciers (Kochtitzky et al., 2022; Recinos et al., 2021). Ice discharge through a flux gate is the closest approximation of frontal ablation (Cogley et al., 2011; Kochtitzky et al., 2022) but excludes ice mass change due to terminus retreat or advance, which is relatively straightforward to measure from terminus delineations, but challenging to predict (Catania et al., 2020).

Greenland Ice Sheet discharge is currently estimated at 487 ± 49 for 2010 to 2017 (Mankoff et al., 2020) and ∼490 Gt a^{-1} from 2006 to 2016 (King et al., 2018). However, these and other estimates are incomplete as they only include the larger, faster glaciers (King et al., 2020; Mankoff et al., 2020; Mouginot et al., 2019; Wood et al., 2021), and thus exclude 77 to 211 ice sheet outlet glaciers, depending on how they are counted, and do not account for peripheral glaciers. While some studies exclude subaerial melt below the fluxgate in discharge estimates (Mouginot et al., 2019), others include it (King et al., 2018; Mankoff et al., 2020), it should not be considered in frontal ablation estimates (Cogley et al., 2011).

The mass balance of the Greenland Ice Sheet has been increasingly negative since the 1980s (Kjeldsen et al., 2015). The Greenland Ice Sheet had a negative mass balance of 285 ± 20 Gt a^{-1} from 2010 to 2018 (Mouginot et al., 2019) and from 1992 to 2018 the contributions of meltwater runoff and ice discharge were approximately equal (Shepherd et al., 2020). However, some of these studies (e.g., Shepherd et al., 2020) use ice discharge to approximate frontal ablation, which double counts some mass loss and does not partition its components in mass balance estimates.

Greenland's marine-terminating glaciers lost a total terminus area of 5,331.9 ± 24.3 km^2 at the ice-ocean interface from 2000 to 2020 (Kochtitzky & Copland, 2022). Of the 745 glaciers that ended in the ocean in 2000, 556 retreated and eight advanced through 2020, with three ice sheet outlets and 71 peripheral glaciers no longer ending in the ocean by 2020 (Kochtitzky & Copland, 2022). The retreat of glaciers in Greenland has typically been accompanied by an increase in flow speed, discharge and loss of mass from those glaciers (King et al., 2020; Rignot & Kanagaratnam, 2006).

Calculating frontal ablation is challenging because glacier termini frequently advance and retreat, necessitating having a fluxgate up-glacier from the calving margin and accounting for terminus mass change. Thus, in addition to ice discharge, we need to compute subaerial melting below the fluxgate and terminus mass changes to ensure subaerial melt is excluded from frontal ablation calculations. Here, we use a suite of model and remote sensing data sets to estimate the frontal ablation for every outlet glacier in Greenland for 2000–2010 and 2010–2020.

2. Results

There were a total of 213 ice sheet outlets and 537 peripheral glaciers in Greenland in the year 2000, compared to 210 and 465, respectively, in the year 2020 (Figure 1; Data Set S1). Even though there are more than twice as many peripheral glaciers, ice sheet outlets contain more than twice the fluxgate length and nearly all the frontal ablation (Table 1), which is a function of their wider calving fronts, larger catchment areas, deeper outlets, and higher flow velocities (Millan et al., 2022; Morlighem et al., 2017). We find a total frontal ablation of 481.8 ± 24.0 for 2000–2010 and 510.2 ± 18.6 Gt a^{-1} for 2010–2020 in Greenland (Table 1). Discharge made up ∼90% of this total during 2000–2010 and 2010–2020 while terminus mass change comprised the remainder (Figure 2). The increase in frontal ablation between the two decades was entirely due to an increase in discharge from 434.5 ± 21.2 to 468.1 ± 15.3 Gt a^{-1}, while terminus mass loss underwent a slight reduction from 47.3 ± 11.3 in 2000–2010 to 42.1 ± 10.6 Gt a^{-1} from 2010 to 2020, although the decrease is within our uncertainty.

The peripheral glaciers made up 1.2% and 0.6% of frontal ablation during 2000–2010 and 2010–2020, respectively (Table 1). The Greenland Ice Sheet alone had a frontal ablation rate of 475.9 ± 31.7 and 507.0 ± 23.0 Gt a^{-1} during 2000–2010 and 2010–2020, respectively, while frontal ablation of peripheral glaciers decreased, within large uncertainties, from 5.9 ± 7.4 to 3.3 ± 4.8 Gt a^{-1} between these periods. The uncertainties larger than the magnitude of change for periphery glaciers is primarily due to highly uncertain thickness data for these glaciers. While terminus mass loss comprised only ∼10% of total Greenland frontal ablation, it was highest in the northeast and northwest during both decades (Figure 1).

Sermeq Kujalleq (Jakobshavn Isbræ) had the largest frontal ablation rate during both decades of 36.3 ± 1.6 and 42.3 ± 1.0 Gt a^{-1} during 2000–2010 and 2010–2020, respectively, with 94% and 99% coming from ice discharge (Figure 2). Ten glaciers accounted for the highest frontal ablation rates during both decades, together comprising

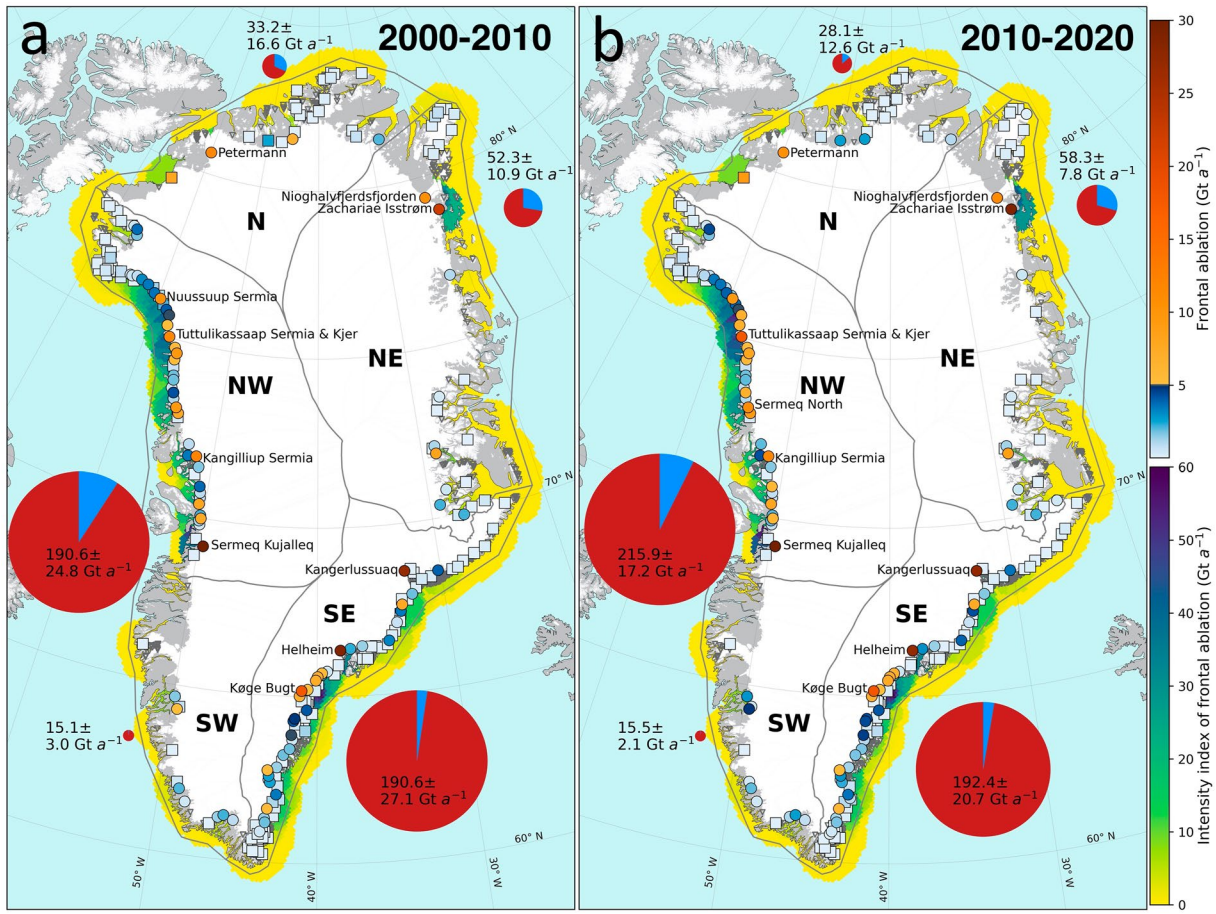

Figure 1. Mean decadal frontal ablation of Greenland for: (a) 2000–2010 and (b) 2010–2020. Sermeq Kujalleq (Jakobshavn Isbræ) is the only glacier with frontal ablation exceeding the blue/red color scale at 36.3 for 2000–2010 and 42.3 Gt a^{-1} for 2010–2020. The graduated circles show the portions of frontal ablation due to terminus mass loss (blue) and ice discharge (red) in each region. Squares indicate glaciers with >50% uncertainty in their frontal ablation estimates and triangles indicate glaciers with <0.02 Gt a^{-1} of frontal ablation. The yellow/green/blue color scale shows the frontal ablation intensity in the ocean for each period, defined as the sum of frontal ablation occurring within 80 km of a glacier terminus. Glacier basins, grouped into five regions, are delineated based on glacier basins from Mouginot and Rignot (2019). Labeled glaciers during each time period are the 10 largest frontal ablation rates in Greenland (Table S1 in Supporting Information S1).

~40.0% of total frontal ablation (Table S1 in Supporting Information S1). Just 17 outlets from 2000 to 2010 and 16 outlets from 2010 to 2020 made up over 50% of total frontal ablation (Table S1 in Supporting Information S1).

Zachariae Isstrøm drains a large portion of the northeast Greenland catchment and is one of the top four glaciers during both decades in terms of total frontal ablation (Table S1 in Supporting Information S1). It lost more than twice the terminus mass of any other glacier in Greenland over the study period, and alone accounted for 24% of total Greenland terminus mass loss from 2000 to 2010, and 35% from 2010 to 2020. Zachariae Isstrøm was one of the top six glaciers during both decades in terms of ice discharge and is the only glacier with high frontal ablation mass losses (top 10) that lost more mass due to terminus mass loss than ice discharge during either period.

To quantify the impact of frontal ablation inputs to the ocean, regardless of the source of the ice, we created a frontal ablation intensity index (Figure 1). We assign each individual glacier's frontal ablation value to marine grid cells within 80 km of its terminus, and sum these values to include frontal ablation from overlapping contributing areas. We choose 80 km to approximate the distance an iceberg can drift in 1–2 weeks, assuming it is not trapped in a fjord (Larsen et al., 2015). Therefore, marine areas with the highest frontal ablation index intensity are found near individual glaciers with high frontal ablation contributions. This index highlights locations where marine environments will potentially be most impacted by direct discharge of icebergs (although frontal ablation is not exactly equal to iceberg volume) within 80 km of outlets and glaciers reaching the ocean. Our index reaches a maximum of about 60 Gt a^{-1} in several areas along the ice sheet margin, including near Tuttulikassaap Sermia (Hayes) & Kjer, Sermeq Kujalleq, Køge Bugt, and Nioghalvfjerdsfjorden.

Table 1
Frontal Ablation for Different Regions in the Northern Hemisphere, and Their Components Due To Ice Discharge and Terminus Mass Change

	Frontal ablation (Gt a^{-1})		Ice discharge (Gt a^{-1})		Terminus mass change (Gt a^{-1})			
	2000–2010	2010–2020	2000–2010	2010–2020	2000–2010	2010–2020	Length of fluxgates (km)	Number of glaciers in 2000
Periphery Greenland	5.9 ± 7.4	3.3 ± 4.8	3.15 ± 7.4	2.31 ± 4.6	−2.77 ± 1.6	−0.99 ± 1.2	854	537
Greenland Ice Sheet	475.9 ± 31.7	507.0 ± 23.0	431.4 ± 30.2	465.8 ± 21.0	−44.5 ± 9.6	−41.1 ± 9.4	2200	213
Total Greenland	481.8 ± 24.0	510.2 ± 18.6	434.5 ± 21.2	468.1 ± 15.3	−47.3 ± 11.3	−42.1 ± 10.6	3,053	750
Northern Hemisphere glaciers outside Greenland	40.2 ± 6.0	48.8 ± 4.5	33.2 ± 5.4	38.5 ± 2.6	−7.0 ± 2.8	−10.3 ± 3.7	3,105	959
Northern Hemisphere glaciers	44.5 ± 6.2	52.0 ± 4.6	35.4 ± 5.4	40.4 ± 2.6	−9.1 ± 3.1	−11.6 ± 3.8	3,802	1,496
Total Northern Hemisphere	522.0 ± 24.8	559.0 ± 19.1	467.7 ± 21.9	506.6 ± 15.5	−54.3 ± 11.6	−52.4 ± 11.2	6,159	1,709

Note. Values for Greenland from this study; values for glaciers outside Greenland from Kochtitzky et al. (2022). All values show net mass loss.

3. Discussion

3.1. Trends in Greenland Frontal Ablation

Greenland frontal ablation increased from 481.8 ± 24.0 for 2000–2010 to 510.2 ± 18.6 Gt a^{-1} for 2010–2020; an increase which has also been noted by other studies in ice discharge (King et al., 2018; Mankoff et al., 2020). Similar to other work, we find that the increase in frontal ablation from 190.6 ± 24.8 to 215.9 ± 17.2 Gt a^{-1} in western Greenland (Figure 1) accounts for nearly all the increase observed in Greenland. To understand what is driving this increase, we examined changes in glacier thickness, velocity, and terminus mass changes, the main variables that control frontal ablation (Cogley et al., 2011; Kochtitzky et al., 2022). We found that the average glacier velocity along the flux gates in this region increased from 280 to 314 m a^{-1} between the decades 2000–2010 and 2010–2020. This 12% increase in glacier velocity is of similar magnitude to the 13% increase in frontal ablation and has implications for glacier evolution and mass loss in the future as this acceleration can drive enhanced mass loss (Aschwanden et al., 2016; Catania et al., 2020).

3.2. Comparison With Previous Estimates of Greenland Ice Discharge

Recent estimates of ice sheet discharge include 487 ± 49 Gt a^{-1} for 2010–2017 (Mankoff et al., 2020), 450 to 550 Gt a^{-1} for 1972–2018 (Mouginot et al., 2019), and ∼490 Gt a^{-1} from 2006 to 2016 (King et al., 2018), although all three studies exclude some ice sheet outlets and all peripheral glaciers. Despite including a larger number of glaciers, we found ice sheet discharge to be 465.8 ± 21.0 Gt a^{-1} for 2010–2020, or ∼6% lower than previous estimates. While within uncertainties, most of this difference is likely due to the location of our fluxgates typically nearer to the terminus than those used in other studies (King et al., 2018; Mankoff et al., 2020), as well as the removal of melt below our fluxgates, as discussed in detail in the following section. Our estimates for peripheral glaciers, which represent about 1% of total Greenland frontal ablation, are within the uncertainties of Kochtitzky et al. (2022) but differ slightly due to modified assumptions about ice velocity, density, and thickness as outlined in the methods section.

3.3. Correction Due To Subaerial Melting

The main difference between previous discharge estimates (King et al., 2018, 2020; Mankoff et al., 2020) and our estimate here is the inclusion of subaerial melting downstream of the fluxgate. While these numbers strongly depend on fluxgate location (i.e., a fluxgate further upstream will result in a higher melt correction), it is useful to review our estimates for comparison to other works. We calculated a mass loss of 17.0 ± 6.8 for 2000–2010 and 14.5 ± 5.8 Gt a^{-1} for 2010–2020 due to subaerial melting after the ice passes through the fluxgate, which is therefore not included in our frontal ablation estimates (Figure S1 in Supporting Information S1). Similarly, terminus mass loss was reduced by 2.4 ± 1.0 for 2000–2010, and 1.6 ± 0.6 Gt a^{-1} for 2010–2020, due to subaerial melting on termini sections that were either lost due to retreat or gained during advance. Because our fluxgates were typically located tens to hundreds of meters lower than those in the similar studies (King et al., 2018; Mankoff et al., 2020), the melt correction for these studies would be higher than values presented herein, although it is beyond the scope of the current study to determine what those values would be.

Our mass loss estimate due to subaerial melting below the fluxgate, thus impacting the discharge term, was lower during 2010–2020 than it was during 2000–2010. This occurred because there was an area loss below the fluxgates of 35% between the two decades, even though the melt rate increased. Thus, the specific melt rate was greater during the later period but applied over a smaller area, resulting in a smaller correction.

3.4. Closing Greenland's Mass Budget

Estimates of the net mass loss of Greenland include 261 ± 43 Gt a^{-1} from satellite gravimetry over 2002–2019 (Velicogna et al., 2020), 222 ± 30 Gt a^{-1} over 2013–2017 (Shepherd et al., 2020), and

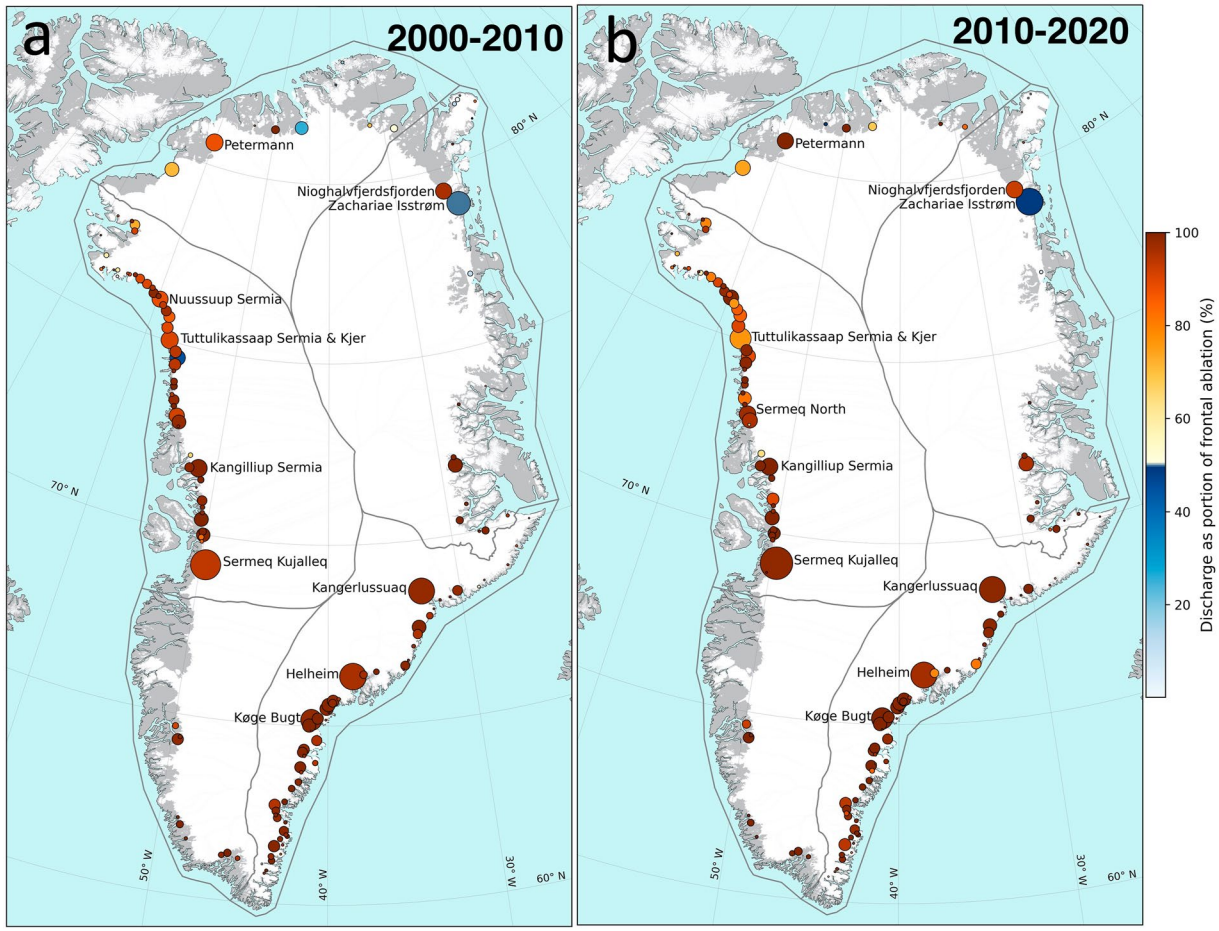

Figure 2. Discharge as total percentage of frontal ablation for: (a) 2000–2010 and (b) 2010–2020. The remaining portion of frontal ablation is due to terminus mass loss (retreat). Larger dots represent more frontal ablation, and the map only shows glaciers with >0.1 Gt a^{-1} of frontal ablation. The absolute values of frontal ablation are shown in Figure 1 for the same periods.

187 ± 17 Gt a^{-1} over 2000–2010 and 286 ± 20 Gt a^{-1} over 2010–2018 (Mouginot et al., 2019). While these estimates come with their own limitations and advantages, our estimates of frontal ablation over a similar period are 220–300 Gt a^{-1} greater than the net mass loss. This suggests a positive climatic-basal mass balance of a similar magnitude attributed primarily to surface accumulation, but possibly with some internal and basal accumulation (Harper et al., 2012).

3.5. Northern Hemisphere Frontal Ablation

Combining our results with those of Kochtitzky et al. (2022), the total frontal ablation for all glaciers that terminate in the ocean in the Northern Hemisphere is 522.0 ± 24.8 for 2000–2010 and 559.0 ± 19.1 Gt a^{-1} for 2010–2020 (Table 1). We combine the results assuming that the uncertainties between estimates of Greenland and that of the other Northern Hemisphere regions are uncorrelated, consistent with both studies. Greenland Ice Sheet discharge, excluding the peripheral glaciers, comprised 83% of total hemispheric frontal ablation in 2000–2010 and 2010–2020. Terminus mass loss in Greenland accounts for 9% in 2000–2010 and 7% in 2010–2020 of Northern Hemisphere frontal ablation. Overall, the Greenland Ice Sheet is by far the largest contributor to frontal ablation in the hemisphere, making up 91% of all frontal ablation during both decades.

4. Conclusions

We present the first estimate of frontal ablation from all marine-terminating ice masses in Greenland, including both outlet glaciers from the ice sheet and peripheral glaciers. There were 213 ice sheet outlets and 537 peripheral glaciers that ended in the ocean in 2000. We found frontal ablation of 481.8 ± 24.0 for 2000–2010

and 510.2 ± 18.6 Gt a^{-1} for 2010–2020, with peripheral glaciers accounting for only 1.2% of frontal ablation in 2000–2010, and 0.6% in 2010–2020. When combined with total mass balance estimates from gravimetry and other methods since 2000, this shows that Greenland had a positive climatic-basal balance, indicating that surface, internal, and basal accumulation exceeds surface, internal, and basal ablation.

We find that discharge made up ∼90% of frontal ablation while terminus mass loss accounts for the remainder, showing the importance of fast outlet glaciers. Sermeq Kujalleq was the largest contributor during both decades with a total frontal ablation of 36.3 ± 0.8 from 2000 to 2010 and 42.3 ± 1.0 Gt a^{-1} from 2010 to 2020, almost all of which came from ice discharge. Zachariae Isstrøm lost more than twice the terminus mass of any other glacier in Greenland during either decade, and is one of the few glaciers to have lost more mass loss from terminus retreat than ice discharge. In all, just 17 glaciers from 2000 to 2010 and 16 glaciers from 2010 to 2020 account for over half the total frontal ablation. These glaciers are the most important to continue monitoring for future impacts on ice sheet mass loss and sea level rise. As a whole, Greenland accounts for 91% of frontal ablation in the Northern Hemisphere.

5. Materials and Methods

Our methods are similar to those described in Kochtitzky et al. (2022), so we describe their core and highlight their differences here. The differences mainly arise from finding a single unified solution to determine changes for periphery glaciers and the ice sheet, as some data sets are only available for one type of glacier in Greenland.

5.1. Estimating Frontal Ablation

To compute frontal ablation, we sum two terms: ice discharge and terminus volume change. Ice discharge is defined as the mass through a fluxgate perpendicular to flow and calculated using the ice velocity and thickness. We compute the terminus volume change from terminus area gained or lost multiplied by the thickness of that area. Changes in ice discharge will contribute to sea level rise, but for terminus volume change only a portion of grounded ice lost during terminus retreat, and ice below water during an advance, will contribute to sea level rise. For all calculations we assume that ice density is 917 kg m^{-3} to be consistent with other estimates from Greenland (King et al., 2018; Mankoff et al., 2020; Mouginot et al., 2019), although this assumption is likely high because the presence of crevasses can only serve to reduce it (Colgan et al., 2016). Crevasses can be common in the terminus region of marine-terminating glaciers, but we lack any information to quantify their number, depth of penetration, or whether they are changing over time. Without this information, and without any direct measurement of the bulk density of ice throughout a glacier, we are unable to provide an assessment of the accuracy of this assumption, consistent with other studies (Colgan et al., 2016; King et al., 2018; Mankoff et al., 2020; Mouginot et al., 2019).

5.2. Identification of Marine-Terminating Glaciers

We manually identified all marine-terminating glaciers in Greenland from Landsat 5, 7, and 8 imagery by mapping those glaciers that touched the ocean in 2000. We use RGI 6.0 (RGI Consortium, 2017) and Mouginot and Rignot (2019) to assign unique identifiers to the periphery and ice sheet glaciers, respectively, to facilitate comparisons with past and future work. We separated periphery and ice sheet glaciers based on the Rastner et al. (2012) connectivity level framework, with periphery glaciers defined as those that had either a weak (CL1) or no (CL0) hydrological connection to the ice sheet while those with a strong connection (CL2) were considered ice sheet outlets in our study. Future work may choose to segregate glaciers differently, which our census approach allows for, and which would not change our total frontal ablation values.

5.3. Ice Discharge

To compute ice discharge, we manually drew 3,053 km of fluxgates approximately perpendicular to flow as close to the terminus of each glacier as practical, preferentially choosing fluxgate locations where ice thickness observations are available from NASA's Operation IceBridge (https://nsidc.org/data/icebridge) flight lines. We then extracted surface velocity and thickness estimates every 25 m (measured using a unique orthographic projection for each glacier) along these fluxgates to compute discharge at each discrete point.

We calculated decadal average glacier surface velocities from optical and synthetic aperture radar (SAR) derived velocity datasets. We used the Inter-mission Time Series of Land Ice Velocity and Elevation (Gardner et al., 2019) and MEaSUREs InSAR (Joughin et al., 2018) for glacier surface velocity estimates. Given that optical velocity mapping is primarily from summer months and SAR derived velocities are primarily from winter months, we combined these data to approximate decadal mean velocity. We assumed that ice velocity at the surface is the same as velocity at the bed, consistent with previous work on Greenland discharge (King et al., 2018; Mankoff et al., 2020). Using the x and y components of velocity from each data source, we corrected the width of the fluxgate to compensate for the drawn fluxgates being oblique to ice flow direction.

To obtain glacier thickness at each point along our fluxgates we preferentially used observations from Operation IceBridge (MacGregor et al., 2021). When those were not available, we used data from BedMachine version 4 (Morlighem et al., 2017). For many periphery glaciers, BedMachine does not include thickness estimates, so for those we use model estimates using a similar shallow ice approximation inversion method from Millan et al. (2022). For small glaciers, when no thickness observations or model results were available, we manually confirmed that the fluxgate is located on the glacier and used a thickness of 30 ± 20 m, lacking any other reasonable estimate. Of these data sources, Operation IceBridge observations covered 9%, BedMachine covered 57%, Millan et al. (2022) covered 33%, and 1% of fluxgate distance was filled with 30 ± 20 m.

5.4. Terminus Volume Change

To quantify frontal ablation due to terminus retreat or advance, we manually digitized the terminus position of each glacier in the study in approximately 2000, 2010, and 2020, based on satellite image availability. We preferentially chose imagery as close as possible to each of these years, first from Landsat 5, 7, and 8, then from ASTER, and finally from Radarsat-1 when no optical imagery was available. We downloaded Landsat imagery from Earth Explorer (earthexplorer.usgs.gov), ASTER imagery from NASA Earth Data (earthdata.nasa.gov), and level-1 Radarsat-1 imagery from the Alaska Satellite Facility (asf.alaska.edu). We reprojected the polygon of each glacier terminus into a unique orthographic coordinate system centered on each polygon for area calculations, to eliminate errors associated with regional projections.

To convert terminus area change into a volume change, we combined the area change observation with the best available thickness data. We first used thickness observations within the terminus area gained or lost, although such observations are only available for 85 glaciers during 2000–2010 and 110 glaciers during 2010–2020. When no observations are available we used Bed Machine version 4 (Morlighem et al., 2017) or Millan et al. (2022) thickness values within the area gained or lost, which covers all remaining glaciers. For unrealistically low glacier thickness values (<30 m), we assumed these reflect errors in the mass conservation modeling and, instead, we used 60% ± 30% of the mean fluxgate thickness for the thickness of area lost for these glaciers. If this was still <30 m, we assumed that the thickness of the area lost was 30 ± 20 m, which is the thickness value we commonly assigned to small peripheral glaciers.

5.5. Surface Mass Balance and Other Adjustments

We used annual surface mass balance estimates from the Regional Atmospheric Climate Model version 2.3p2 (RACMO2.3p2) at 5.5 km, statistically downscaled to 1 km resolution (Noël et al., 2019) from 2000 to 2019 to determine the climatic mass balance for each glacier in order to account for subaerial melting once mass has passed through the fluxgate but before it calves. We applied the climatic mass balance rate to half of each decadal terminus area change to represent the mean terminus position over each period, which assumes a linear retreat rate over each decade. We then subtract that from the terminus mass loss. We do the same for the portion of the glacier below the flux gate but above the most retreated terminus position of the decade being considered.

To account for changes in ice thickness along a fluxgate during the study period, we used geodetic mass balance estimates from Hugonnet et al. (2021) for 2000–2019, which includes all locations within 10 km of a peripheral glacier. Thus, we also used this data set for 74% of the ice sheet outlet glacier flux gate points. When these data were not available (36% of ice sheet fluxgate points), we used geodetic mass balance estimates from Khan et al. (2016, 2022) for outlet glaciers.

While we used the same corrections to debias the data as described in Kochtitzky et al. (2022), there are small differences. We found a bias of 43 m (model ice is too thin) when comparing observations from Operation

IceBridge along our fluxgates and BedMachine version 4 (Morlighem et al., 2017). We examined how this bias correlated with depth, but did not find a linear relationship, as exists with data from Millan et al. (2022). Thus, we are not able to debias Bed Machine results, but we do debias data from Millan et al. (2022), as described in Kochtitzky et al. (2022).

5.5.1. Error Analysis

Our error analysis mirrors that of Kochtitzky et al. (2022) We used the stated uncertainties available with the velocity (Gardner et al., 2019), thickness (MacGregor et al., 2021; Millan et al., 2022; Morlighem et al., 2017), surface mass balance (Noël et al., 2019), and geodetic mass balance (Khan et al., 2016, 2022) data sets. We report all uncertainties at 2-sigma confidence, unless otherwise specified. We determined the uncertainty of our manual digitization of glacier termini by multiplying the perimeter of each polygon by the pixel resolution (30 m for Landsat, 15 m for ASTER, 8 m for Radarsat-1 fine beam mode) of each type of imagery used (Krumwiede et al., 2014). To examine the spatial correlation of velocity and thickness uncertainties, we used global-scale, empirical variograms (Mälicke & Schneider, 2019; Matheron, 1965), testing the spatial autocorrelation from 25 m to 1,000 km. Ultimately, we used these variograms to propagate uncertainties from pixel-scale to glacier- and region-wide, for both ice discharge and terminus mass change contributions to frontal ablation.

The error analysis here differs from Kochtitzky et al. (2022) by scaling velocity and ice thickness errors reported in the input datasets to match those from a cross-comparison of available data. We found empirical errors 3 times larger than those reported for ice thickness (2.7 for velocity) on average over Greenland, and thus scaled all errors by multiplying with these factors. This step was not necessary in Kochtitzky et al. (2022) owing to a good agreement over the Northern Hemisphere, on average. In Greenland, these larger errors might originate from difficulties in measuring or modeling thicker ice or estimating ice velocity. Consequently, there is a large difference in reported uncertainties for peripheral glacier between this study and Kochtitzky et al. (2022). Studies focusing on the periphery of Greenland should use estimates from Kochtitzky et al. (2022) instead of the results presented here.

Data Availability Statement

Fluxgates, attributes at points along the fluxgates, and final frontal ablation estimates for each glacier can be found at the Polar Data Catalogue data set 13272 (https//doi.org/10.21963/13272). The scripts used in this work can be found at github.com/willkochtitzky/FrontalAblation (version used in this publication updated on 23 June 2022, commit 81d076c).

Acknowledgments
WK acknowledges support from the Vanier Graduate Scholarship. LC thanks the Natural Sciences and Engineering Research Council of Canada, University of Ottawa, and ArcticNet Network of Centres of Excellence Canada for funding. MK acknowledges support from the National Aeronautics and Space Administration (NASA), Grant 80NSSC22K1709, and the University of Washington Applied Physics Lab SEED program. HJ acknowledges support from the Natural Sciences and Engineering Research Council of Canada.

References

Aschwanden, A., Fahnestock, M. A., & Truffer, M. (2016). Complex Greenland outlet glacier flow captured. *Nature Communications*, *7*, 1–8. https://doi.org/10.1038/ncomms10524

Catania, G. A., Stearns, L. A., Moon, T. A., Enderlin, E. M., & Jackson, R. H. (2020). Future evolution of Greenland's marine-terminating outlet glaciers. *Journal of Geophysical Research: Earth Surface*, *125*(2), 1–28. https://doi.org/10.1029/2018JF004873

Cogley, J. G., Hock, R., Rasmussen, L. A., Arendt, A. A., Bauder, A., Braithwaite, R. J., et al. (2011). Glossary of glacier mass balance and related terms (p. 86). IHP-VII Technical Documents in Hydrology No.

Colgan, W., Rajaram, H., Abdalati, W., McCutchan, C., Mottram, R., Moussavi, M. S., & Grigsby, S. (2016). Glacier crevasses: Observations, models, and mass balance implications. *Reviews of Geophysics*, *54*(1), 119–161. https://doi.org/10.1002/2015RG000504

Fettweis, X., Hofer, S., Krebs-Kanzow, U., Amory, C., Aoki, T., Berends, C. J., et al. (2020). GrSMBMIP: Intercomparison of the modelled 1980-2012 surface mass balance over the Greenland Ice Sheet. *The Cryosphere*, *14*(11), 3935–3958. https://doi.org/10.5194/tc-14-3935-2020

Gardner, A. S., Fahnestock, M. A., & Scambos, T. A. (2019). *ITS_LIVE regional glacier and ice sheet surface velocities*. Data archived at National Snow and Ice Data Center. https://doi.org/10.5067/6II6VW8LLWJ7

Goelzer, H., Nowicki, S., Payne, A., Larour, E., Seroussi, H., Lipscomb, W. H., et al. (2020). The future sea-level contribution of the Greenland Ice Sheet: A multi-model ensemble study of ISMIP6. *The Cryosphere*, *14*(9), 3071–3096. https://doi.org/10.5194/tc-14-3071-2020

Harper, J., Humphrey, N., Pfeffer, W. T., Brown, J., & Fettweis, X. (2012). Greenland ice-sheet contribution to sea-level rise buffered by meltwater storage in firn. *Nature*, *491*(7423), 240–243. https://doi.org/10.1038/nature11566

Hugonnet, R., McNabb, R., Berthier, E., Menounos, B., Nuth, C., Girod, L., et al. (2021). Accelerated global glacier mass loss in the early twenty-first century. *Nature*, *592*, 726–731. https://doi.org/10.1038/s41586-021-03436-z

IPCC. (2021). In V. P. Masson-Delmotte, A. Zhai, S. L. Pirani, C. Connors, S. Péan, N. Berger. et al. (Eds.), *Climate Change 2021: The Physical Science Basis. Contribution of Working Group I to the Sixth Assessment Report of the Intergovernmental Panel on Climate Change*. Cambridge University Press. https://doi.org/10.1017/9781009157896

Joughin, I., Smith, B., Howat, I., & Scambos, T. (2018). *MEaSUREs Greenland ice sheet velocity map from InSAR data, version 2*. NASA National Snow and Ice Data Center Distributed Active Archive Center. https://doi.org/10.5067/OC7B04ZM9G6Q

Karlsson, N. B., Solgaard, A. M., Mankoff, K. D., Gillet-Chaulet, F., MacGregor, J. A., Box, J. E., et al. (2021). A first constraint on basal melt-water production of the Greenland Ice Sheet. *Nature Communications*, *12*(1), 1–10. https://doi.org/10.1038/s41467-021-23739-z

Khan, S. A., Bamber, J. L., Rignot, E., Helm, V., Aschwanden, A., Holland, D. M., et al. (2022). Greenland mass trends from airborne and satellite altimetry during 2011-2020. *Journal of Geophysical Research: Earth Surface*, *127*(4), 1–20. https://doi.org/10.1029/2021jf006505

Khan, S. A., Sasgen, I., Bevis, M., Van Dam, T., Bamber, J. L., Willis, M., et al. (2016). Geodetic measurements reveal similarities between post–Last Glacial Maximum and present-day mass loss from the Greenland ice sheet. *Science Advances*, *2*(9), e1600931. https://doi.org/10.1126/sciadv.1600931

King, M. D., Howat, I. M., Candela, S. G., Noh, M. J., Jeong, S., Noël, B. P. Y., et al. (2020). Dynamic ice loss from the Greenland ice sheet driven by sustained glacier retreat. *Communications Earth & Environment*, *1*(1), 1–7. https://doi.org/10.1038/s43247-020-0001-2

King, M. D., Howat, I. M., Jeong, S., Noh, M. J., Wouters, B., Noël, B., & Van Den Broeke, M. R. (2018). Seasonal to decadal variability in ice discharge from the Greenland ice sheet. *The Cryosphere*, *12*(12), 3813–3825. https://doi.org/10.5194/tc-12-3813-2018

Kjeldsen, K. K., Korsgaard, N. J., Bjørk, A. A., Khan, S. A., Box, J. E., Funder, S., et al. (2015). Spatial and temporal distribution of mass loss from the Greenland ice sheet since AD 1900. *Nature*, *528*(7582), 396–400. https://doi.org/10.1038/nature16183

Kochtitzky, W., & Copland, L. (2022). Retreat of northern hemisphere marine-terminating glaciers, 2000–2020. *Geophysical Research Letters*, *49*(3), 1–10. https://doi.org/10.1029/2021gl096501

Kochtitzky, W., Copland, L., Van Wychen, W., Hugonnet, R., Hock, R., Dowdeswell, J. A., et al. (2022). The unquantified mass loss of Northern Hemisphere marine-terminating glaciers from 2000-2020. *Nature Communications*, *13*(1), 5835. https://doi.org/10.1038/s41467-022-33231-x

Krumwiede, B. S., Kamp, U., Leonard, G. J., Kargel, J. S., Dashtseren, A., & Walther, M. (2014). Recent glacier changes in the Mongolian Altai Mountains: Case studies from Munkh Khairkhan and Tavan Bogd. In R. B. Kargel, G. J. Leonard, M. Bishop, & A. Kääb (Eds.), *Global land ice measurements from space* (pp. 481–508). Springer. https://doi.org/10.1007/978-3-540-79818-7_22

Larsen, P.-H., Hansen, M. O., Buus-Hinkler, J., Krane, K. H., & Sønderskov, C. (2015). Field tracking (GPS) of ten icebergs in eastern Baffin Bay, offshore Upernavik, northwest Greenland. *Journal of Glaciology*, *61*(227), 421–437. https://doi.org/10.3189/2015JoG14J216

MacGregor, J. A., Boisvert, L. N., Medley, B., Petty, A. A., Harbeck, J. P., Bell, R. E., et al. (2021). The scientific legacy of NASA's operation IceBridge. *Reviews of Geophysics*, *59*(2), e2020RG000712. https://doi.org/10.1029/2020RG000712

Mälicke, M., & Schneider, H. D. (2019). Scikit-GStat 0.2.6: A scipy flavored geostatistical analysis toolbox written in Python. https://doi.org/10.5281/ZENODO.3531816

Mankoff, K. D., Solgaard, A., Colgan, W., Ahlstrøm, A. P., Khan, S. A., & Fausto, R. S. (2020). Greenland Ice Sheet solid ice discharge from 1986 through March 2020. *Earth System Science Data*, *12*(2), 1367–1383. https://doi.org/10.5194/essd-12-1367-2020

Matheron, G. (1965). *Les variables régionalisées et leur estimation. Une application de la théorie des fonctions aléatoires aux sciences de la nature*. Masson et Cie.

Millan, R., Mouginot, J., Rabatel, A., & Morlighem, M. (2022). Ice velocity and thickness of the world's glaciers. *Nature Geoscience*, *15*(2), 124–129. https://doi.org/10.1038/s41561-021-00885-z

Morlighem, M., Williams, C. N., Rignot, E., An, L., Arndt, J. E., Bamber, J. L., et al. (2017). BedMachine v3: Complete bed topography and ocean bathymetry mapping of Greenland from Multibeam echo sounding combined with mass conservation. *Geophysical Research Letters*, *44*(21), 11051–11061. https://doi.org/10.1002/2017GL074954

Mouginot, J., & Rignot, E. (2019). Glacier catchments/basins for the Greenland ice sheet. *Dryad*. https://doi.org/10.7280/D1WT11

Mouginot, J., Rignot, E., Bjørk, A. A., van den Broeke, M., Millan, R., Morlighem, M., et al. (2019). Forty-six years of Greenland ice sheet mass balance from 1972 to 2018. *Proceedings of the National Academy of Sciences of the United States of America*, *116*(19), 9239–9244. https://doi.org/10.1073/pnas.1904242116

Noël, B., van de Berg, W. J., Lhermitte, S., & van den Broeke, M. R. (2019). Rapid ablation zone expansion amplifies north Greenland mass loss. *Science Advances*, *5*(9), 2–11. https://doi.org/10.1126/sciadv.aaw0123

Noël, B., van de Berg, W. J., van Wessem, J. M., van Meijgaard, E., van As, D., Lenaerts, J. T. M., et al. (2018). Modelling the climate and surface mass balance of polar ice sheets using RACMO2 - Part 1: Greenland (1958-2016). *The Cryosphere*, *12*(3), 811–831. https://doi.org/10.5194/tc-12-811-2018

Rastner, P., Bolch, T., Mölg, N., Machguth, H., Le Bris, R., & Paul, F. (2012). The first complete inventory of the local glaciers and ice caps on Greenland. *The Cryosphere*, *6*(6), 1483–1495. https://doi.org/10.5194/tc-6-1483-2012

Recinos, B., Maussion, F., Noël, B., Möller, M., & Marzeion, B. (2021). Calibration of a frontal ablation parameterisation applied to Greenland's peripheral calving glaciers. *Journal of Glaciology*, *67*(266), 1177–1189. https://doi.org/10.1017/jog.2021.63

RGI Consortium. (2017). Randolph Glacier inventory – A dataset of global glacier outlines: Version 6.0. Boulder, Colorado, USA. NSIDC: National Snow and Ice Data Center. https://doi.org/10.7265/4m1f-gd79

Rignot, E., & Kanagaratnam, P. (2006). Changes in the velocity structure of the Greenland ice sheet. *Science*, *311*(5763), 986–990. https://doi.org/10.1126/science.1121381

Shepherd, A., Ivins, E., Rignot, E., Smith, B., van den Broeke, M., Velicogna, I., et al. (2020). Mass balance of the Greenland ice sheet from 1992 to 2018. *Nature*, *579*(7798), 233–239. https://doi.org/10.1038/s41586-019-1855-2

Velicogna, I., Mohajerani, Y., Geruo, A., Landerer, F., Mouginot, J., Noel, B., et al. (2020). Continuity of ice sheet mass loss in Greenland and Antarctica from the GRACE and GRACE follow-on missions. *Geophysical Research Letters*, *47*(8). https://doi.org/10.1029/2020GL087291

Wood, M., Rignot, E., Fenty, I., An, L., Bjørk, A., van den Broeke, M., et al. (2021). Ocean forcing drives glacier retreat in Greenland. *Science Advances*, *7*(1), 1–11. https://doi.org/10.1126/sciadv.aba7282